

## ChILD: A Pictorial Review of Pulmonary Imaging Findings in Childhood Interstitial Lung Diseases

Nupur Verma, MD<sup>a</sup>, Stephan Altmayer, MD<sup>b</sup>, Bruno Hochhegger, MD, PhD<sup>b</sup>,  
Mariane Cibelle Barros, MD<sup>c</sup>, Dhanashree Rajderkar, MD<sup>a</sup>,  
Tan-Lucien Mohammed, MD, FCCP<sup>a,\*</sup>

<sup>a</sup> Department of Radiology, University of Florida College of Medicine, Gainesville, FL

<sup>b</sup> Department of Radiology, Pontificia Universidade Catolica do Rio Grande do Sul, Porto Alegre, Brazil

<sup>c</sup> Department of Radiology, Hospital Moinhos de Vento, Porto Alegre, Brazil

### ABSTRACT

Childhood interstitial lung disease (chILD) is a group of lung disorders characterized by lung remodeling leading to abnormal gas exchange. ChILD is classified differently from adult interstitial lung disease and encompasses 2 broad categories: “disorders more prevalent in infancy” (<2 years) and “disorders not specific to infancy” (>2 years). High-resolution computed tomography can play an important role in the evaluation of chILD by narrowing the differential diagnosis and preventing unnecessary invasive procedures if typical imaging patterns are recognized. Thus, the pediatric radiologist should consider chILD in children with respiratory distress and identify the imaging patterns to suggest the diagnosis.

© 2020 Elsevier Inc. All rights reserved.

### Introduction

Childhood interstitial lung diseases (chILD) are an uncommon set of lung disorders characterized by remodeling of the lung parenchyma leading to abnormal gas exchange.<sup>1</sup> ChILD natural history and etiology differ from adult presentation of interstitial lung diseases (ILD).<sup>1,2</sup> Although there is some overlap in the histopathologic pathologic patterns of ILD in children and adults, they occur in different proportions and some diseases are unique to each age group.<sup>2,3</sup> Thus, chILD is classified differently from adult ILD to avoid confusion regarding nomenclature, etiology, and prognosis.<sup>1,2</sup> ChILD is classified together as a group as they often present overlapping clinical (cough, tachypnea, and hypoxemia) and imaging features (eg, diffuse abnormalities on radiography). Grouping facilitates the identification of a phenotype that warrants prompt diagnostic evaluation and treatment to allay pulmonary damage.<sup>1</sup>

The most widely used classification of chILD was published by the chILD Research Network in 2007, which was recently endorsed by the American Thoracic Society.<sup>1,2</sup> Although the classification system is based on clinical and histopathologic characteristics, it emphasizes the importance of age as the primary organizing parameter because of the unique disorders affecting young children. As a result, the classification scheme is divided in 2 broad categories: “disorders more prevalent in infancy” (<2 years) and “disorders not specific to infancy” (>2 years). High-resolution computed tomography (HRCT) can play an important

role in the evaluation of chILD by narrowing the differential diagnosis and avoiding invasive procedures for diagnosis if typical imaging patterns are recognized. The objective of this article is to review the HRCT imaging patterns associated with the chILD spectrum and how imaging can play a role in the diagnostic work-up of these disorders.

### Differential Diagnosis Based on HRCT Findings

The recognition of the various patterns of abnormality seen on HRCT is important in the evaluation of patients with chILD to characterize the nature and distribution of the disease.<sup>1</sup> Various patterns of abnormality have been described in the literature, which sometimes are overlapped. However, some HRCT patterns of ILD can sometimes narrow the differential diagnosis or even suggest a specific diagnosis, improving diagnostic accuracy. As a result, HRCT findings in the right clinical context may help clinicians to avoid subsequent invasive testing, such as in Neuroendocrine hyperplasia of infancy (NEHI) and surfactant dysfunction mutations (SDM),<sup>1,4–7</sup> identify the site of highest yield for biopsy,<sup>1</sup> among other advantages as highlighted in [Table 1](#). Below, we discuss the most common HRCT imaging patterns observed in chILD. A summary of the imaging findings associated with each chILD disease herein discussed is provided in [Table 2](#).

#### Ground-Glass Attenuation

Ground-glass attenuation (GGA) is defined as an increased attenuation of the lung parenchyma without obscuration of the pulmonary vascular markings on CT images.<sup>8</sup> There are several chILD conditions mainly characterized by diffuse GGA in infancy, especially NEHI and

Funding: None.

\*Reprint requests: Tan-Lucien Mohammed, MD, FCCP, Department of Radiology, University of Florida College of Medicine, Post Office Box 100374, Gainesville, FL 32610

E-mail address: [mohtan@radiology.ufl.edu](mailto:mohtan@radiology.ufl.edu) (T.-L. Mohammed).

<https://doi.org/10.1067/j.cpradiol.2020.03.003>

0363-0188/© 2020 Elsevier Inc. All rights reserved.

**TABLE 1**  
Advantages of HRCT in the care of patients with chILD syndrome

Avoid unnecessary lung biopsy if typical imaging findings are present (eg, NEHI, BO, HP)
Suggest appropriate laboratorial tests to avoid invasive procedures (eg, SDM)
Narrow down the differential diagnosis of chILD if imaging is nonspecific
Estimate clinical severity of the disease (eg, bronchopulmonary dysplasia)
Identify higher yield biopsy targets

SDM. This pattern is also very prevalent in chILD of older children. Hypersensitivity pneumonitis (HP) manifests with diffuse ground-glass opacification in 73% in the acute phase.<sup>9</sup> Additionally, connective tissue disease (CTD)-related lung disease could show diffuse GGA in patients with nonspecific interstitial pneumonia (NSIP) and lymphocytic pneumonia.

#### Reticulation, Cysts, and Traction Bronchiectasis/Bronchiolectasis

Reticular pattern demonstrated by septal thickening on imaging may reflect the presence of pulmonary fibrosis. Other signs of fibrosis include distortion of the pulmonary architecture, traction bronchiectasis and bronchiolectasis, and cysts.<sup>10</sup> Chronic ILD that most often have a reticular pattern include chronic neonatal lung disease, pulmonary interstitial glycogenosis (PIG), SDM (especially beyond infancy), chronic HP, and CTD-related lung disease.

#### Bronchiectasis and Air Trapping

Bronchiectasis is irreversible localized or diffuse bronchial dilatation, usually resulting from chronic infection, proximal airway obstruction, or congenital bronchial abnormality.<sup>11</sup> Morphologic criteria on thin-section CT scans include bronchial dilatation with respect to the accompanying pulmonary artery (signet-ring sign), lack of tapering of bronchi, and identification of bronchi within 1 cm of the pleural surface.<sup>11</sup> Air trapping is defined as areas of decreased attenuation during end-expiration and lack of volume reduction.<sup>8</sup> Air trapping is commonly seen in NEHI and bronchiolitis obliterans (BO), but the presence of central bronchiectasis and bronchial wall thickening is only typical of BO. Also, chronic aspiration may also show bronchiectasis bilaterally, especially in the lower lung zones.

**TABLE 2**  
Differential diagnoses and radiological features of childhood interstitial lung diseases

	What to expect on CT	Take-home points
Lung growth abnormalities	Decreased size and perfusion of the affected lung (pulmonary hypoplasia), large areas of decreased attenuation with linear and subpleural opacities (BPD), subpleural cysts (Down syndrome)	Imaging is often sufficient for evaluating etiology, biopsy is only performed if symptoms are disproportionate to clinical context
Pulmonary interstitial glycogenosis	Bilateral GGA and consolidations, septal thickening, cystic lesions	Highly associated with LGA due to prematurity and with CHD. Biopsy is necessary to confirm the diagnosis
Neuroendocrine hyperplasia of infancy	Bilateral central GGA (RML and lingula > upper lungs), diffuse air-trapping with mosaic attenuation	No need for biopsy if typical CT findings in the right clinical context
Surfactant deficiency	Diffuse GGA (decreases with age), cystic lesions (increase with aging), septal thickening	Highly associated with congenital malformations (CHD > GI > renal). Consider genetic tests if adequate clinical suspicion (imaging increases suspicion)
Alveolar capillary dysplasia	Diffuse bilateral GGA, septal thickening, prominence of pulmonary vessels (due to pulmonary hypertension)	Consider FOFX1 testing if available, otherwise lung biopsy is required for diagnosis
Bronchiolitis obliterans	Mosaic attenuation with bronchial wall thickening/bronchiectasis	Typical CT findings in the right clinical context may obviate the need for lung biopsy
Connective tissue disease-associated lung disease	Variable	Laboratorial and history findings often sufficient to make the diagnosis of CTD-related ILD. Biopsy is rarely necessary.
Lysosomal storage diseases	Ground-glass attenuation, interlobular septal thickening, cysts and nodules	Associated with findings of multiple-organ involvement, especially hepatosplenomegaly
Cryptogenic organizing pneumonia	Multiple GGA or consolidation (bilateral and peripheral), but may also present as unifocal opacity	Biopsy is necessary to confirm the diagnosis. CT helps to locate the site of highest yield for biopsy.
Hypersensitivity pneumonitis	Acute/subacute: bilateral GGA, small centrilobular opacities, air trapping Chronic: reticulation, traction bronchiectasis, areas of honeycombing	CT findings in the right clinical context is often sufficient for an accurate non-invasive diagnosis

CHD, congenital heart disease; GI, gastrointestinal.

## Diseases More Prevalent in Infancy

### Lung Growth Abnormalities

Lung growth abnormalities (LGA) are among the most common etiologies of infant ILD.<sup>12</sup> The several entities of LGA that can be broadly categorized into chronic lung disease of prematurity (formerly bronchopulmonary dysplasia, BPD), pulmonary hypoplasia (due to in utero effusion, mass compression, thoracic dysplasia, congenital diaphragmatic hernia, and oligohydramnios), genetic conditions (particularly trisomy 21), and congenital heart disease. They also show features of tachypnea, hypoxemia, retractions, and diffuse radiographic abnormalities. Radiological findings are variable as they depend mainly on the etiology, age of the infant, and severity of the LGA.

CT would show the growth anomalies, such as pulmonary and vascular hypoplasia, and the resultant decreased size and perfusion of the affected lung. **Figure 1** demonstrates a case of right pulmonary hypoplasia associated with proximal interruption of the right pulmonary artery. Trisomy 21 is associated with the presence of peripheral subpleural cysts that most often involve the anteromedial portion of the lungs<sup>13</sup> (**Fig 2**). Patients with BPD commonly show large areas of decreased attenuation corresponding to alveolar enlargement and reduced distal vascularization, linear and subpleural triangular opacities, bronchial wall thickening, and bullae (**Fig 3**).<sup>14–16</sup> The severity of lung function and respiratory symptoms is correlated to higher scores of CT abnormalities in patients with BPD.<sup>14</sup>

Imaging is helpful in evaluating the possible cause of infants with LGA presenting with respiratory dysfunction early in life, which makes lung biopsy generally unnecessary. Patients referred for biopsy are those who typically have pulmonary symptoms disproportionate to their clinical circumstances.<sup>2</sup> For instance, patchy PIG is a common concurrent histologic finding in infants with LGA, as discussed below.

### Pulmonary Interstitial Glycogenosis

PIG is an idiopathic disorder related to abnormal lung development that results in the accumulation of glycogen and lipid-containing mesenchymal cells consistent with lipofibroblasts.<sup>17</sup> These infants typically present with persistent tachypnea and hypoxemia usually since birth but or within the first month of life.<sup>18–20</sup> This condition is highly



**FIG 1.** A 1-month-old child with right pulmonary hypoplasia associated with right pulmonary artery agenesis. (A) Chest radiography depicted an important right-sided volume loss with rightward mediastinal shift. (B) Contrast-enhanced axial HRCT demonstrated right pulmonary volume loss and proximal interruption of the right pulmonary artery (arrow). (C) Three-dimensional reconstruction of the heart and great vessels showing proximal interruption of the right pulmonary artery (arrow).

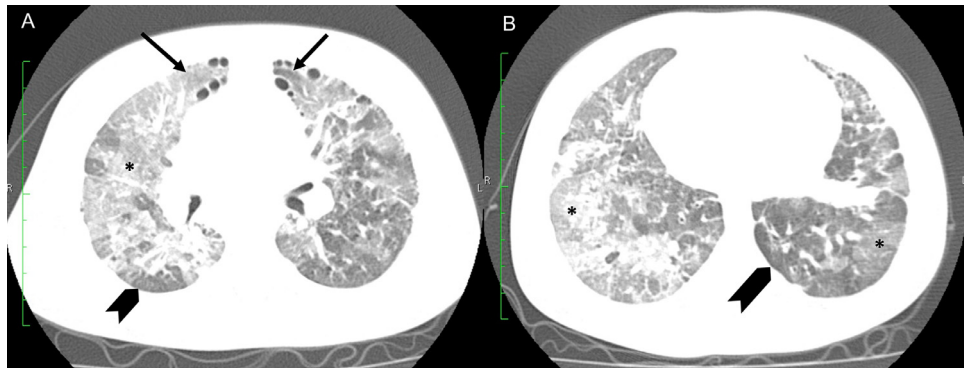


**FIG 2.** An 18-month-old patient with pulmonary hypoplasia associated with Down syndrome. (A, B) Axial HRCT reveals several subpleural cysts located in the anteromedial portion of both lungs (arrows). Diffuse ground-glass attenuation (asterisks) intermixed with hyperlucent areas due to perfusion defects (arrowheads) and linear opacities are also observed.



**FIG 3.** An 8-month-old patient born at 25 weeks of gestation and a history of recurrent pulmonary infections. (A, B) Axial HRCT reveals areas of decreased attenuation (asterisks), linear opacities (arrows), and subpleural triangular-shaped opacities (arrowheads).

associated with a spectrum of pulmonary and extrapulmonary disorders, such as LGA due to prematurity and congenital heart defects, supporting the theory of a development abnormality.<sup>19,20</sup> Radiography in PIG shows hyperinflation of the lungs and diffuse infiltrates or hazy opacities.<sup>18</sup> Most common CT findings are diffuse bilateral GGA, consolidations, interlobular septal thickening, and cystic lesions (Fig 4).<sup>19-21</sup> The diagnosis can only be made at lung biopsy, as imaging findings alone are not specific enough to confirm the diagnosis.<sup>18,19</sup>

*Genetic Disorders of Surfactant Dysfunction*

Surfactant deficiency is the leading cause of respiratory distress syndrome (RDS) in newborns; which is primarily caused by preterm delivery of infants with an immature lung and inadequate surfactant

activity. Another cause of RDS is related to SDM in genes encoding proteins for normal surfactant metabolism. Full-term newborns with SDM may manifest with severe RDS that resembles the presentation of a preterm infant with an immature lung.<sup>1</sup> These SDM involve member A3 of ATP binding cassette family of transporters (locus ABCA3), surfactant proteins B and C (locus SFTPB and SFTPC, respectively) and thyroid transcription Factor 1 (TTF-1, locus NKX2.1).<sup>1</sup> The clinical presentation of infants with each of these mutations is variable. While children with SFTPB mutation usually have progressive fatal RDS shortly after birth,<sup>22</sup> carriers of the ABCA3, SFTPC, and NKX2.1 mutation have a more variable presentation, from severe neonatal diffuse lung disease to chronic ILD later in life.<sup>7,22,23</sup>

Early imaging findings of SDM resemble those of RDS, characterized by GGAs that are either diffuse throughout the lungs or patchy



**FIG 4.** A 34-week premature infant evaluated at 14 days-of-life for persistent tachypnea and grunting. (A) Chest radiography shows diffuse interstitial opacities bilaterally. (B) Axial HRCT revealed diffuse ground-glass attenuation and patchy consolidations around the right middle and right lower lobar bronchi. (C) Coronal minimum intensity projection (MinIP) reconstruction showed several small ovoid radiolucencies bilaterally (arrows). Lung biopsy confirmed the diagnosis of pulmonary interstitial glycogenosis.

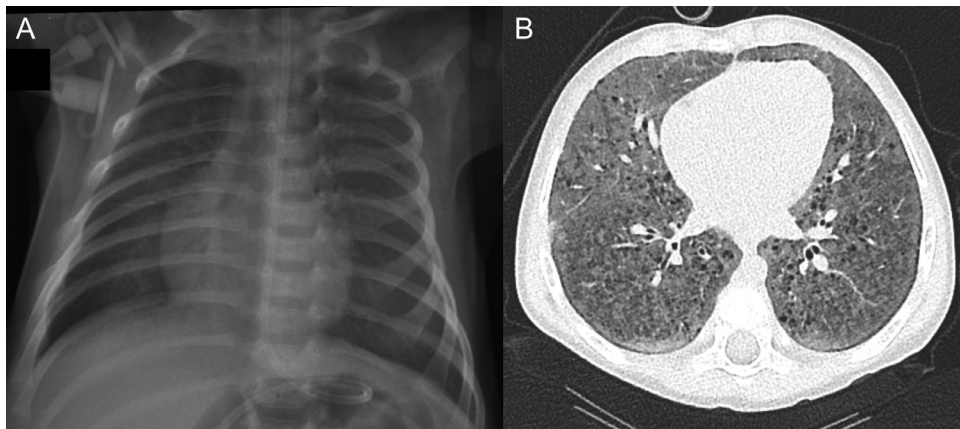


**FIG 5.** Full-term newborn evaluated for surfactant dysfunction mutation due to a history of respiratory distress at birth and persistent symptoms. (A) Chest radiography performed at 2 weeks of age shows nonspecific, faint interstitial opacities bilaterally. (B) Axial HRCT at 18 months of age revealed diffuse ground-glass attenuation bilaterally, interstitial septal thickening, and several cystic lesions in the parenchyma.

but involving multiple lobes.<sup>7,24,25</sup> The extent of GGA decreases with age, but patients develop interlobular septal thickening and parenchymal lung cysts that increase in number and size over time (Fig 5).<sup>7,25</sup> Patients presenting beyond infancy may have significant architectural and fibrotic changes (Fig 6). Interestingly, pectus excavatum was seen in all patients of a cohort with ABCA3 who were imaged beyond infancy.<sup>7</sup> It is worth noting that children with NKX2.1 often have associated congenital hypothyroidism and neurologic abnormalities (eg, chorea, ataxia), which may be clues toward the differential diagnosis.<sup>23,26</sup> As mentioned before, typical imaging findings in a patient with clinical suspicion of SDM may obviate the need for invasive procedures due to the availability of genetic testing for these mutations.<sup>1</sup>

#### Neuroendocrine Cell Hyperplasia of Infancy

Neuroendocrine cell hyperplasia of infancy (NEHI) typically presents with persistent tachypnea, retractions, and hypoxia usually before the first year of life.<sup>27,28</sup> Findings on chest radiography are often nonspecific and mimic those of viral illness, such as lung hyperinflation and perihilar opacities.<sup>27-29</sup> Conversely, HRCT findings are very distinctive with centrally distributed GGA, preferentially involving the right middle lobe and lingula, and diffuse air trapping with mosaic attenuation on expiratory images (not always available; Fig 7).<sup>4</sup> Consolidations are observed in up to 20% of cases, and also have a preferentially central distribution.<sup>4</sup> The central distribution of the GGA in NEHI helps to distinguish it from other conditions that

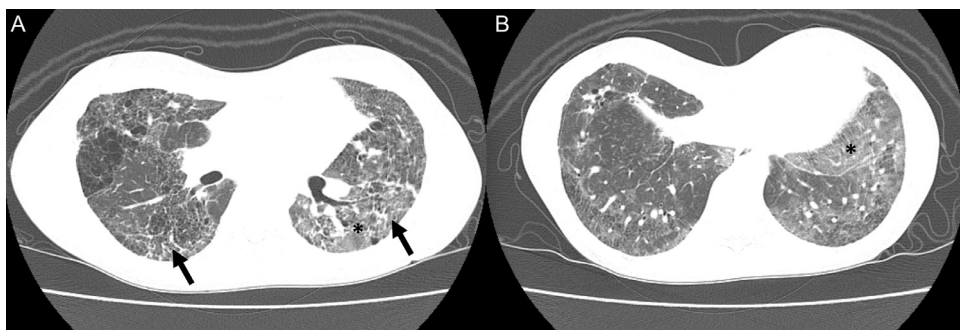


**FIG 6.** A 10-year-old patient diagnosed later in childhood with surfactant deficiency due to ABCA3 mutation. (A, B) Axial HRCT demonstrates areas of ground-glass attenuation (asterisks) with interlobular septal thickening (arrows) and severe lung architectural distortion. Note the presence of a pectus excavatum deformity, a typical finding of children with ABCA3 with late presentation.

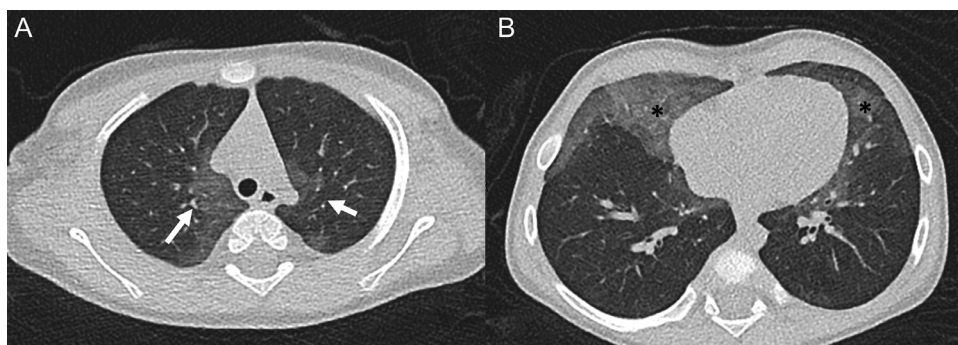


**FIG 7.** A 6-month-old patient with persistent tachypnea diagnosed with neuroendocrine cell hyperplasia of infancy. (A, B) Axial HRCT shows areas of ground-glass attenuation in the bilateral perimedial areas of the superior lobes (arrows). (B) Ground-glass attenuation was also observed in the right middle lobe and lingula (asterisks).

present with GGA and air trapping, such as BO and SDM.<sup>4</sup> However, the former is primarily distinguished by the presence of prominent central bronchiectasis, and the latter by more diffusely distributed GGAs (rather than central as in NEHI) and the presence of interlobular septal thickening.

Lung biopsy revealing an increased number of neuroendocrine cells by bombesin immunostaining was historically considered the gold standard for NEHI diagnosis.<sup>28</sup> However, given the high specificity of the HRCT findings of NEHI, the 2015 American Thoracic Society guidelines now support the noninvasive diagnosis of NEHI based on HRCT findings and compatible clinical context.<sup>1,6</sup> NEHI has a prolonged course with eventual improvement at a mean age of 5 years with the use of oxygen supplementation.<sup>27</sup>

#### Alveolar Capillary Dysplasia With Misalignment of the Pulmonary Veins

It has been hypothesized that alveolar capillary dysplasia with misalignment of the pulmonary veins arises from an antenatal insult to the fetal lung vascularization, resulting in a reduced number of pulmonary capillaries and blood drainage through anomalous (“misaligned”) veins.<sup>30</sup> ACD-MPV presents with severe hypoxemic respiratory failure and pulmonary hypertension in full-term infants with nearly uniform mortality in the first month of life.<sup>1,31</sup> The presentation may resemble that of persistent pulmonary hypertension of the newborn, except that ACD-MPV typically does not respond to general supportive care. Additionally, ACD-MPV is often associated with cardiac, genitourinary, and cardiac malformations, such as patent ductus arteriosus, hypoplastic left heart, and ventricular septal defect.<sup>32</sup> Radiographs may show diffuse haziness and scattered bilateral GGAs.<sup>30,33</sup> On CT, ACD-MPV presents with diffuse bilateral GGA with extensive interlobular septal thickening.<sup>31,33,34</sup>

Atypical cases of ACD-MPV presenting outside the neonatal period (usually before 6 months of age) with progressive hypoxemia and signs of idiopathic pulmonary hypertension have been reported in

the literature.<sup>31,34,35</sup> Thus, this condition should be suspected even in children beyond the neonatal period presenting with idiopathic pulmonary hypertension, congenital malformations, and typical CT findings.<sup>31</sup> The presence of diffuse GGA and interlobular septal thickening on chest CT can be helpful to distinguish ACD-MPV from other causes of idiopathic pulmonary hypertension in infancy. Definitive diagnosis is based on abnormalities of the pulmonary vasculature on lung biopsy or autopsy. However, approximately 60%-80% of newborns with ACD-MPV were identified with mutations involving the *FOXF1* gene,<sup>31,32</sup> which could be tested to avoid the need for lung biopsy.<sup>1</sup> Imaging may play an important role in supporting clinical suspicion, especially in late presenters.

#### Diseases More Prevalent in Children

##### Bronchiolitis Obliterans

BO is a chronic obstructive lung disease most frequently related to an antecedent lower respiratory tract infection. The predominant cause of postinfectious BO in children is *Adenovirus*.<sup>36</sup> However, other causes of BO have been established, such as chronic rejection of lung transplantation, and graft-vs-host disease associated with bone marrow.<sup>5,37</sup> Histologically, BO is characterized by fibroproliferative thickening of the bronchial walls leading to concentric narrowing of the airways and sometimes complete luminal obliteration.<sup>38</sup>

BO manifests as dyspnea and airflow limitation not reversible with the use of inhaled bronchodilators.<sup>37</sup> Chest radiography is often normal, but may show hyperinflation, persistent atelectasis, or bronchial wall thickening.<sup>39</sup> Characteristic HRCT findings of BO are mosaic pattern of attenuation, air trapping, GGA, bronchial wall thickening, and central bronchiectasis (Fig 8).<sup>39</sup> Centrilobular nodules and atelectasis are also present in around 20%-30% of patients.<sup>5</sup> These findings, especially the diffuse pattern of mosaic attenuation, are particularly useful for distinguishing BO from severe asthma in children with obstructive pulmonary disease that do not demonstrate the typical

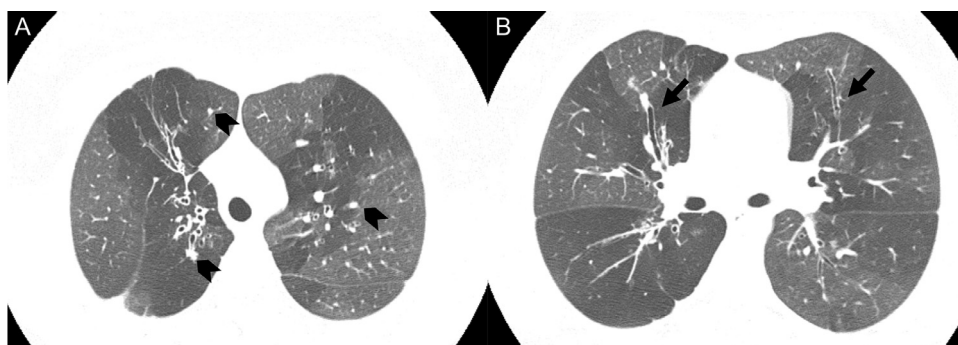


**FIG 8.** Follow-up scan of a 13-year-old with a history of severe adenovirus infection at age 5. (A, B) HRCT demonstrates areas of mosaic pattern of attenuation, bronchiectasis (arrows), and centrilobular nodules (arrowheads) bilaterally. HRCT findings were compatible with postinfectious bronchiolitis obliterans.

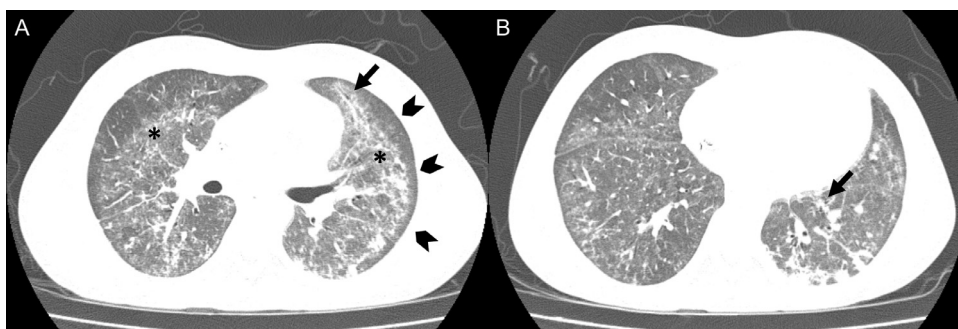


**FIG 9.** A 14-year-old patient presenting with dyspnea on exertion. (A, B) Axial HRCT demonstrates diffuse areas of ground-glass attenuation (asterisks) with subpleural sparing (arrowheads), interlobular septal thickening, and sparse traction bronchiectasis (arrows). Histologic evaluation was compatible with nonspecific interstitial pneumonia.

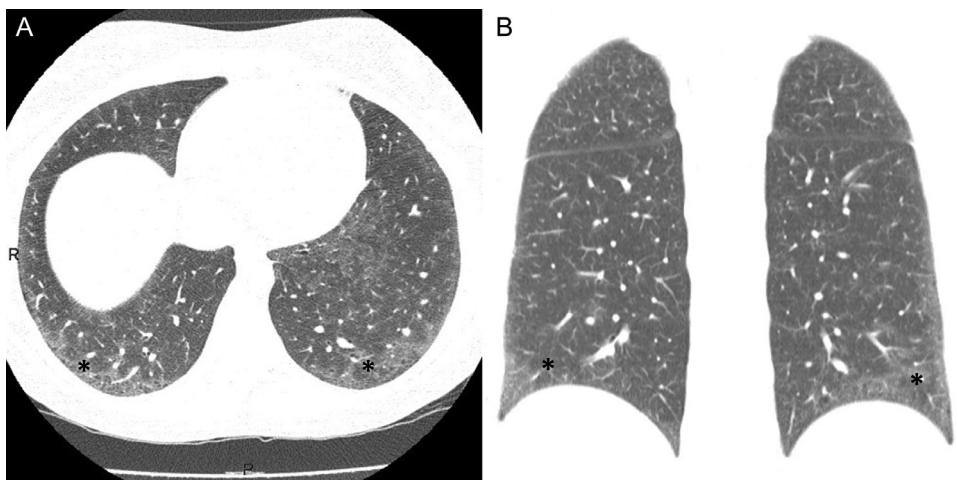


**FIG 10.** A 16-year-old female diagnosed with HIV and Sjögren's syndrome presenting with chronic cough. (A, B) Axial and coronal HRCT demonstrate centrilobular nodules and ground-glass attenuation predominantly in the lower lobes (asterisks). Histologic diagnosis revealed the diagnosis of lymphocytic interstitial pneumonitis.

reversible response to bronchodilators.<sup>5</sup> Additionally, the findings of bronchiectasis and distribution of areas of increased attenuation help differentiating BO from other conditions with mosaic attenuation, such as NEHI and SDM. Thus, the presence of those typical CT findings in the right clinical context may obviate the need for open lung biopsy.<sup>5,39</sup>

#### CTD-Associated Interstitial Lung Disease

CTD-associated ILDs are often encountered in older children and underlie a significant proportion of the chILD beyond infancy.<sup>3,40</sup> Pulmonary disease onset may precede or be associated with the concurrent systemic illness similar to adults, including systemic lupus erythematosus (SLE), juvenile dermatomyositis, systemic sclerosis, juvenile idiopathic arthritis, to name a few.<sup>41</sup> Patterns of lung involvement and radiological findings at presentation are variable and certain patterns of lung involvement are recognized with increased frequency in each CTD.<sup>42</sup> For instance, juvenile dermatomyositis rarely manifests as ILD in children, differently from adult dermatomyositis in which symptomatic lung involvement occurs in more than half of the patients.<sup>42</sup> Conversely, systemic sclerosis more often presents with ILD in children than in adults.<sup>41</sup> In a study by Soares et al, only 35% of children with an ILD underwent a lung biopsy; the remaining were classified based on clinical history, serologic testing, and imaging.<sup>40</sup> Thus, whenever one of the CTD patterns of pulmonary disease is found on a child, a diligent search of an underlying CTD is always warranted, especially because it may present before the systematic symptoms manifest.

Children with SLE develop pulmonary disease less often than adults.<sup>41</sup> Pleuritis with or without pleural effusion is the most common pulmonary manifestation of SLE. Acute lupus pneumonitis is a

rare but life-threatening condition characterized by fever and respiratory distress with diffuse bilateral interstitial and alveolar infiltrates on imaging.<sup>43,44</sup> ILD occurs in less than 10% of SLE, with the most common histologic pattern is nonspecific interstitial pneumonia (NSIP).<sup>41,44</sup> In contrast to SLE, more than half of children with systemic sclerosis presents with any form ILD, and NSIP appears to be the most common histologic appearance.<sup>41,45,46</sup> Typical HRCT findings of NSIP include peripheral GGA with variable reticular opacities that predominates in the lower lobes (Fig 9).<sup>46,47</sup> Other imaging findings, including traction bronchiectasis, subpleural nodules, and even honeycombing are also reported.<sup>46,47</sup> Only 10%–20% of children with dermatomyositis and polymyositis are found to have an ILD; they most often present with NSIP or pattern similar to cryptogenic organizing pneumonia (COP). Children with Sjogren's syndrome are more likely to present with CT findings of lymphocytic interstitial pneumonitis compared to other CTDs (Fig 10).<sup>41</sup>

#### Lysosomal Storage Diseases

Lysosomal storage diseases (LSDs) are a large group of conditions caused most part by lysosomal enzyme deficiencies leading to a build-up of undegraded substrates.<sup>48</sup> Gaucher disease is the most common LSDs and is grouped within the sphingolipidoses (lipid storage disease) along with Fabry and Niemann–Pick disease.<sup>49</sup> The manifestation of the sphingolipidoses is related to the accumulation of lipid-laden macrophages in spleen, liver, bones, brain, and also lung. Pulmonary involvement occurs with the infiltration of these cells in the alveolar space leading to disruption of the surfactant production and progressive inflammatory response in the alveoli.<sup>50,51</sup>

Radiological features of LSDs usually include bilateral pulmonary infiltrates (mostly interstitial, but also alveolar, or mixed) that can be

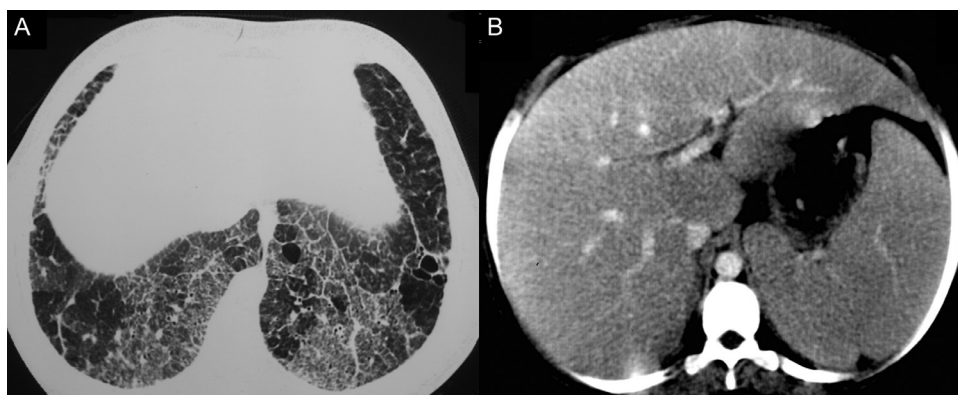


**FIG 11.** A 9-year-old boy with Niemann-Pick disease presenting with chronic cough. (A) Axial HRCT revealed extensive areas of “crazy paving” pattern in both lower lobes. (B) Imaging of the abdomen showed severe hepatosplenomegaly, compatible with the diagnosis of Niemann-Pick.



**FIG 12.** A 17-year-old female diagnosed with HIV and Sjögren's syndrome diagnosed with subacute hypersensitivity pneumonitis due to exposure to birds. (A) Coronal inspiratory HRCT demonstrate diffuse areas of ground-glass attenuation bilaterally. (B) Axial expiratory HRCT shows hyperlucent areas surrounded by normal attenuated lung to air trapping. (C) Follow-up axial HRCT one year after removal of the exposed antigen.

reticular, nodular, reticulonodular, or even honeycombing. HRCT helps characterize the disease pattern and other findings suggestive of ILD, such as interlobular septal thickening, GGA, cysts, and nodules (Fig 11).<sup>52</sup> Radiological findings of LSDs are heterogeneous, and the radiologist must rely on other clinical (eg, hepatosplenomegaly) and history findings to consider the diagnosis of LSD-related ILD.

#### Hypersensitivity Pneumonitis

HP is also known as extrinsic allergic alveolitis and is more frequently diagnosed in school-age children, with a mean age of presentation of 10 years.<sup>41</sup> HP results from an immune reaction to inspired organic particles, which is most often related to bird antigens, but also associated with exposure to mold, pesticides, or chemicals,

including aerosolized epoxies and volatile compounds.<sup>41,53</sup> The presentation of the acute form of HP occurs hours after the initial exposure to the antigen and may be confused with a viral illness; symptoms include cough, fever, dyspnea, and malaise that diminishes over the next 24 hours.<sup>53</sup> In the subacute form, children gradually develop a chronic cough, low-grade fever, hypoxemia, and crackles on auscultation in up to 50% of patients. With disease progression to chronic HP, children may remain with chronic cough, fatigue, and exercise intolerance.<sup>41,53</sup>

Imaging findings are variable, and there is a significant overlap in the imaging findings of each of the 3 stages of disease.<sup>54,55</sup> In acute/subacute pulmonary hypertension often shows patchy or diffuse bilateral GGA and small centrilobular nodular ground-glass opacities (usually <5 mm; Fig 12).<sup>56</sup> Areas of normal extensive GGA

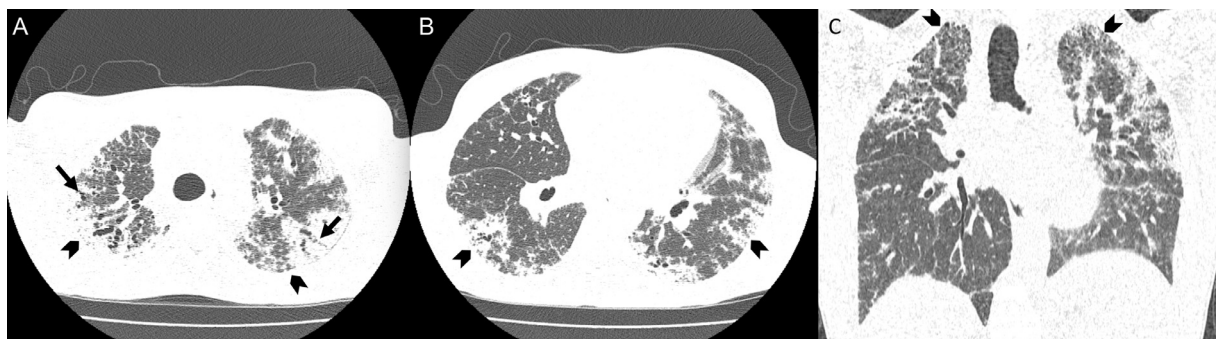


**FIG 13.** A 12-year-old boy with a history of chronic exposure to bat droppings presenting with cough and dyspnea on exertion. (A, B) Axial HRCT images show extensive areas of honeycombing (arrowheads), interlobular septal thickening, and traction bronchiectasis (arrows) in both superior lobes. (C) Coronal HRCT image depicts the predominance of the fibrotic changes in the superior lobes. Histopathologic diagnosis demonstrated noncaseous granulomas and giant cells of peribronchovascular distribution, compatible with the diagnosis of hypersensitivity pneumonitis.

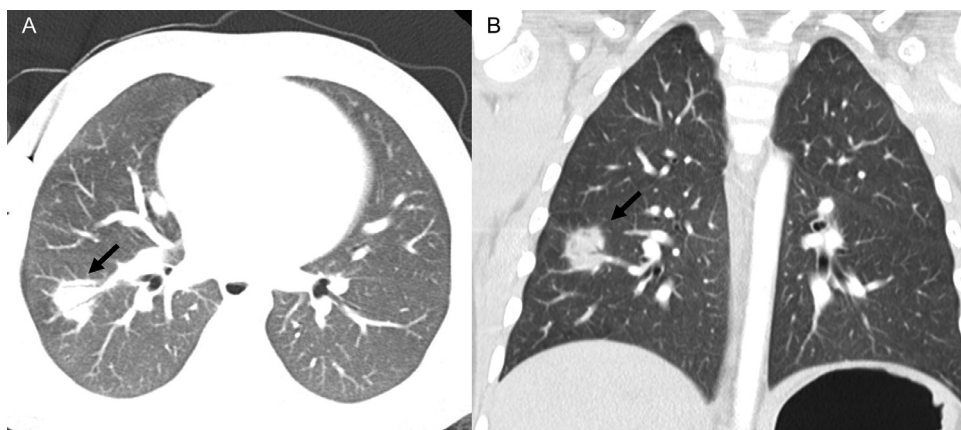


**FIG 14.** A 5-year-old boy with diagnosis of neuroblastoma presenting with persistent nonproductive cough. (A, B) Axial and coronal HRCT revealed a focal consolidation in the superior segment of the right inferior lobe (arrows). Histopathologic diagnosis was compatible with cryptogenic organizing pneumonia.

intercalated with air trapping and normal lung, known as the “head cheese sign,” are also observed, particularly in the subacute phase.<sup>9,57</sup> In the chronic phase, the predominant findings are reticular opacities, interlobular septal thickening, traction bronchiectasis with architectural distortion, and some cases result in honeycombing similar to an HRCT pattern of usual interstitial pneumonia (Fig 13).<sup>56,57</sup> Reaching the diagnosis is dependent on a suspicious environmental history with demonstration of exposure coinciding with the disease, laboratory results, and imaging findings compatible with HP.<sup>41,53</sup>

#### Cryptogenic Organizing Pneumonia

COP, which was previously known as BO organizing pneumonia, is the idiopathic form of organizing pneumonia, which affects the distal airways and alveoli.<sup>58</sup> Organizing (secondary) pneumonia may also be associated with acute infection, transplant, and medications, as well as autoimmune diseases and the cryptogenic form is exceeding rare in children.<sup>58</sup> Therefore, careful evaluation for secondary causes of ILD should be performed before suspecting COP, including viral and mycoplasma illnesses. Pathogenesis has been attributed to ongoing inflammation, and therefore the use of anti-inflammatory drugs in the treatment of this condition can be helpful. Clinical presentation is often with flu-like illness with progressive and unresolving dyspnea.<sup>58</sup> Anorexia and weight loss often accompany the illness.

The predominant imaging pattern of COP is areas of consolidation or GGA that are usually multiple (but may also be unifocal), located mainly in the subpleural and peribronchovascular regions, and often migratory (Fig 14).<sup>59,60</sup> Air bronchograms and mild bronchial dilation are also common within the consolidations.<sup>55</sup> As the imaging findings of COP are nonspecific, this consolidative imaging pattern in children should be differentiated from lymphoma, eosinophilic pneumonia, and sarcoidosis. Lung biopsy may be necessary to make the diagnosis. COP may resolve spontaneously, but response to steroids is very favorable with improvement within days of week in both imaging and symptoms.<sup>61</sup>

#### Conclusion

ChILD are uncommon in comparison to adult presentation, but with increased awareness of their etiologies and typical imaging findings, they are being diagnosed more frequently. In the setting of early infancy (<2 years), congenital etiology should be strongly considered, as opposed to presentation in toddlers and school-age children when environmental, CTD-related, and immunologic disorders are more likely to be the etiology. The radiologist can play an essential role in the diagnostic work-up, particularly in the “disorders more prevalent in infancy,” as typical imaging patterns may obviate the need for

invasive lung biopsy for many of the conditions. Even if the imaging appearance is nonspecific, the radiologist can still contribute to narrow the differential diagnosis and identify potentially higher yield biopsy targets.

#### References

1. Kurland G, Deterding RR, Hagood JS, et al. An official American Thoracic Society Clinical Practice Guideline: Classification, evaluation, and management of childhood interstitial lung disease in infancy. *Am J Respir Crit Care Med* 2013;188:376–94. [Internet].
2. Deutsch GH, Young LR, Deterding RR, et al. Diffuse lung disease in young children. *Am J Respir Crit Care Med* 2007;176:1120–8. [Internet].
3. Fan LL, Dishop MK, Galambos C, et al. Children's interstitial and diffuse lung disease research network (chILD). Diffuse lung disease in biopsied children 2 to 18 years of age. Application of the chILD classification scheme. *Ann Am Thorac Soc* 2015;12:1498–505. [Internet].
4. Brody AS, Guillerman RP, Hay TC, et al. Neuroendocrine cell hyperplasia of infancy: Diagnosis with high-resolution CT. *AJR Am J Roentgenol* 2010;194:238–44. [Internet].
5. Jensen S, Lynch D, Brown K, et al. High-resolution CT features of severe asthma and bronchiolitis obliterans. *Clin Radiol* 2002;57:1078–85. [Internet].
6. Young LR, Brody AS, Inge TH, et al. Neuroendocrine cell distribution and frequency distinguish neuroendocrine cell hyperplasia of infancy from other pulmonary disorders. *Chest* 2011;139:1060–71. [Internet].
7. Doan ML, Guillerman RP, Dishop MK, et al. Clinical, radiological and pathological features of ABCA3 mutations in children. *Thorax* 2008;63:366–73. [Internet].
8. Hansell DM, Bankier AA, MacMahon H, et al. Fleischner society: Glossary of terms for thoracic imaging. *Radiology* 2008;246:697–722. [Internet].
9. Griese M, Haug M, Hartl D, et al. Hypersensitivity pneumonitis: Lessons for diagnosis and treatment of a rare entity in children. *Orphanet J Rare Dis* 2013;8:121. [Internet].
10. Elicker B, de Castro Pereira CA, Webb R, et al. Padrões tomográficos das doenças intersticiais pulmonares difusas com correlação clínica e patológica. *J Bras Pneumol* 2008;34:715–44. [Internet].
11. Milliron B, Henry TS, Veerarahavan S, et al. Bronchiectasis: Mechanisms and imaging clues of associated common and uncommon diseases. *Radiographics* 2015;35:1011–30. [Internet].
12. Das S, Langston C, Fan LL. Interstitial lung disease in children. *Curr Opin Pediatr* 2011;23:325–31. [Internet].
13. Biko DM, Schwartz M, Anupindi SA, et al. Subpleural lung cysts in Down syndrome: Prevalence and association with coexisting diagnoses. *Pediatr Radiol* 2008;38:280–4. [Internet].
14. van Mastrigt E, Logie K, Ciet P, et al. Lung CT imaging in patients with bronchopulmonary dysplasia: A systematic review. *Pediatr Pulmonol* 2016;51:975–86. [Internet].
15. Spagnolo P, Bush A. Interstitial lung disease in children younger than 2 years. *Pediatrics* 2016;137:e20152725. [Internet].
16. Mahut B, De Blic J, Emond S, et al. Chest computed tomography findings in bronchopulmonary dysplasia and correlation with lung function. *Arch Dis Child Fetal Neonatal Ed* 2007;92:F459–64. [Internet].
17. Deutsch GH, Young LR. Lipofibroblast phenotype in pulmonary interstitial glycogenosis. *Am J Respir Crit Care Med* 2016;193:694–6. [Internet].
18. Canakis A-M, Cutz E, Manson D, et al. Pulmonary interstitial glycogenosis: A new variant of neonatal interstitial lung disease. *Am J Respir Crit Care Med* 2002;165:1557–65. [Internet].
19. Seidl E, Carlens J, Reu S, et al. Pulmonary interstitial glycogenosis—A systematic analysis of new cases In: *Rare ILD/DPLD Eur Respir Soc* 2018;140:11–20.



20. Cutz E, Chami R, Dell S, et al. Pulmonary interstitial glycogenosis associated with a spectrum of neonatal pulmonary disorders. *Hum Pathol* 2017;68:154–65. [Internet].
21. Weinman JP, White CJ, Liptzin DR, et al. High-resolution CT findings of pulmonary interstitial glycogenosis. *Pediatr Radiol* 2018;48:1066–72. [Internet].
22. Noguee LM. Alterations in SP-B and SP-C expression in neonatal lung disease. *Annu Rev Physiol* 2004;66:601–23. [Internet].
23. Doyle DA, Gonzalez I, Thomas B, et al. Autosomal dominant transmission of congenital hypothyroidism, neonatal respiratory distress, and ataxia caused by a mutation of NKX2-1. *J Pediatr* 2004;145:190–3. [Internet].
24. Newman B, Kuhn JP, Kramer SS, et al. Congenital surfactant protein B deficiency—Emphasis on imaging. *Pediatr Radiol* 2001;31:327–31. [Internet].
25. Amin RS, Wert SE, Baughman RP, et al. Surfactant protein deficiency in familial interstitial lung disease. *J Pediatr* 2001;139:85–92. [Internet].
26. Iwatani N, Mabe H, Devriendt K, et al. Deletion of NKX2.1 gene encoding thyroid transcription factor-1 in two siblings with hypothyroidism and respiratory failure. *J Pediatr* 2000;137:272–6. [Internet].
27. Deterding RR, Pye C, Fan LL, et al. Persistent tachypnea of infancy is associated with neuroendocrine cell hyperplasia. *Pediatr Pulmonol* 2005;40:157–65. [Internet].
28. O'Connor MG, Wurth M, Young LR. Rare becomes more common: Recognizing neuroendocrine cell hyperplasia of infancy in everyday pulmonary consultations. *Ann Am Thorac Soc* 2015;12:1730–2. [Internet].
29. Gomes V.C.C., Silva M.C.C., Maia Filho J.H., et al. Diagnostic criteria and follow-up in neuroendocrine cell hyperplasia of infancy: A case series. *J Bras Pneumol* 2013;39:569–78. [Internet].
30. Bishop NB, Stankiewicz P, Steinhorn RH. Alveolar capillary dysplasia. *Am J Respir Crit Care Med* 2011;184:172–9. [Internet].
31. Towe CT, White FV, Grady RM, et al. Infants with atypical presentations of alveolar capillary dysplasia with misalignment of the pulmonary veins who underwent bilateral lung transplantation. *J Pediatr* 2018;194:158–64. [Internet]e1.
32. Szafranski P, Gambin T, Dharmadhikari AV, et al. Pathogenetics of alveolar capillary dysplasia with misalignment of pulmonary veins. *Hum Genet* 2016;135:569–86. [Internet].
33. Szafranski P, Dharmadhikari AV, Wambach JA, et al. Two deletions overlapping a distant FOXF1 enhancer unravel the role of lncRNA LINC01081 in etiology of alveolar capillary dysplasia with misalignment of pulmonary veins. *Am J Med Genet A* 2014;164:2013–9. [Internet].
34. Ito Y, Akimoto T, Cho K, et al. A late presenter and long-term survivor of alveolar capillary dysplasia with misalignment of the pulmonary veins. *Eur J Pediatr* 2015;174:1123–6. [Internet].
35. Shankar V, Haque A, Johnson J, et al. Late presentation of alveolar capillary dysplasia in an infant. *Pediatr Crit Care Med* 2006;7:177–9. [Internet].
36. Colom AJ, Teper AM, Vollmer WM, et al. Risk factors for the development of bronchiolitis obliterans in children with bronchiolitis. *Thorax* 2006;61:503–6. [Internet].
37. Moonnumakal SP, Fan LL. Bronchiolitis obliterans in children. *Curr Opin Pediatr* 2008;20:272–8. [Internet].
38. Visscher DW, Myers JL. Bronchiolitis: The pathologist's perspective. *Proc Am Thorac Soc* 2006;3:41–7. [Internet].
39. Champs NS, Lasmar LM, Camargos PA, et al. Post-infectious bronchiolitis obliterans in children. *J Pediatr (Rio J)* 2011;87:187–98. [Internet].
40. Soares JJ, Deutsch GH, Moore PE, et al. Childhood interstitial lung diseases: An 18-year retrospective analysis. *Pediatrics* 2013;132:684–91. [Internet].
41. Vece TJ, Fan LL. Interstitial lung disease in children older than 2 years. *Pediatr Allergy Immunol Pulmonol* 2010;23:33–41. [Internet].
42. Dell S, Cernelc-Kohan M, Hagood JS. Diffuse and interstitial lung disease and childhood rheumatologic disorders. *Curr Opin Rheumatol* 2012;24:530–40. [Internet].
43. Şişmanlar Eyüboğlu T, Aslan AT, Özdemir Y, et al. Isolated acute lupus pneumonitis as the initial presentation of systemic lupus erythematosus in an 8-year-old girl. *Autoimmun Highlights* 2018;9:4. [Internet].
44. Beresford MW, Cleary AG, Sills JA, et al. Cardio-pulmonary involvement in juvenile systemic lupus erythematosus. *Lupus* 2005;14:152–8. [Internet].
45. Bouros D, Wells AU, Nicholson AG, et al. Histopathologic subsets of fibrosing alveolitis in patients with systemic sclerosis and their relationship to outcome. *Am J Respir Crit Care Med* 2002;165:1581–6. [Internet].
46. Seely JM, Jones LT, Wallace C, et al. Systemic sclerosis: Using high-resolution CT to detect lung disease in children. *Am J Roentgenol* 1998;170:691–7. [Internet].
47. Valeur NS, Stevens AM, Ferguson MR, et al. Multimodality thoracic imaging of juvenile systemic sclerosis: Emphasis on clinical correlation and high-resolution CT of pulmonary fibrosis. *Am J Roentgenol* 2015;204:408–22. [Internet].
48. Sun A. Lysosomal storage disease overview. *Ann Transl Med* 2018;6:476. [Internet].
49. Meikle PJ. Prevalence of lysosomal storage disorders. *JAMA* 1999;281:249. [Internet]A.
50. Griese M, Brasch F, Aldana V, et al. Respiratory disease in Niemann-Pick type C2 is caused by pulmonary alveolar proteinosis. *Clin Genet* 2010;77:119–30. [Internet].
51. Paget TL, Parkinson-Lawrence EJ, Orgeig S. Interstitial lung disease and surfactant dysfunction as a secondary manifestation of disease: Insights from lysosomal storage disorders. *Drug Discov Today Dis Model* 2019;29:35–42. [Internet].
52. Semple T, Owens CM. The radiology of diffuse interstitial pulmonary disease in children: Pearls, pitfalls and new kids on the block in 2015. *Radiol Med* 2016;121:352–61. [Internet].
53. Fan LL. Hypersensitivity pneumonitis in children. *Curr Opin Pediatr* 2002;14:323–6. [Internet].
54. Lacasse Y, Selman M, Costabel U, et al. Classification of hypersensitivity pneumonitis. *Int Arch Allergy Immunol* 2009;149:161–6.
55. Guilleman RP. Imaging of childhood interstitial lung disease. *Pediatr Allergy Immunol Pulmonol* 2010;23:43–68.
56. Tateishi T, Ohtani Y, Takemura T, et al. Serial high-resolution computed tomography findings of acute and chronic hypersensitivity pneumonitis induced by avian antigen. *J Comput Assist Tomogr* 2011;35:272–9.
57. Silva CIS, Chung A, Müller NL. Hypersensitivity pneumonitis: Spectrum of high-resolution CT and pathologic findings. *Am J Roentgenol* 2007;188:334–44.
58. Cordier J-F. Cryptogenic organising pneumonia. *Eur Respir J* 2006;28:422–46.
59. Lee KS, Kullnig P, Hartman TE, et al. Cryptogenic organizing pneumonia: CT findings in 43 patients. *Am J Roentgenol* 1994;162:543–6.
60. Faria IM, Zanetti G, Barreto MM, et al. Organizing pneumonia: Chest HRCT findings. *J Bras Pneumol* 2015;41:231–7.
61. Lee JW, Lee KS, Lee HY, et al. Cryptogenic organizing pneumonia: Serial high-resolution CT findings in 22 patients. *Am J Roentgenol* 2010;195:916–22.